

Experimental investigation of GafChromic[®] EBT3 intrinsic energy dependence with kilovoltage x rays, ¹³⁷Cs, and ⁶⁰Co

Cliff G. Hammer^{a)}

Department of Medical Physics, School of Medicine and Public Health, University of Wisconsin-Madison, Madison, WI 53705, USA

Benjamin Saul Rosen

Department of Radiation Oncology, University of Michigan, Ann Arbor, MI 48109, USA

Jessica M. Fagerstrom

Northwest Medical Physics Center, Lynnwood, WA 98036, USA

Wesley S. Culberson and Larry A. DeWerd

Department of Medical Physics, School of Medicine and Public Health, University of Wisconsin-Madison, Madison, WI 53705, USA

(Received 30 August 2017; revised 13 October 2017; accepted for publication 7 November 2017; published 22 December 2017)

Purpose: To determine experimentally the intrinsic energy response, k_{bq} , of EBT3 GafChromic[®] radiochromic film with kilovoltage x rays, ¹³⁷Cs, and ⁶⁰Co in therapeutic and diagnostic dose ranges through direct measurement with an accompanying mathematical approach to describe the physical processes involved.

Methods: The EBT3 film was irradiated with known doses using ⁶⁰Co, ¹³⁷Cs, and 13 NIST-matched kilovoltage x-ray beams. Seven dose levels, ranging from 57 to 7002 mGy, were chosen for this work. Monte Carlo methods were used to convert air-kerma rates to dose rates to the film active layer for each energy. A total of 738 film dosimeters, each measuring $(1.2 \times 1.2) \text{ cm}^2$, were cut from three film sheets out of the same lot of the latest version of EBT3 film, to allow for multiple dosimeters to be irradiated by each target dose and beam quality as well as unirradiated dosimeters to be used as controls. Net change in optical density in excess of the unirradiated controls was measured using the UWMRRC Laser Densitometry System (LDS). The dosimeter intrinsic energy response, k_{bq} , for each dose level was determined relative to ⁶⁰Co, as the ratio of dosimeter response to each beam quality relative to the absorbed dose to the film active volume at the same dose level. A simplified, single-hit mathematical model was used to derive a single-free-parameter, β , which is a proportionality constant that is dependent on beam quality and describes the microdosimetric interactions within the active layer of film. The response of β for each beam quality relative to ⁶⁰Co was also determined.

Results: k_{bq} was determined for a wide range of doses and energies. The results show a unique variation of k_{bq} as a function of energy, and agree well with results from other investigations. There was no measurable dose dependence for k_{bq} within the 500–7002 mGy range outside of the expanded measurement uncertainty of 3.65% ($k = 2$). For doses less than 500 mGy, the signal-to-noise ratio was too low to determine k_{bq} accurately. The single-free-parameter, β , fit calculations derived from the single-hit model show a correlation with k_{bq} that suggests that β , at least in part, characterizes the microdosimetric interactions that determine k_{bq} .

Conclusions: For the beam qualities investigated, a single energy-dependent k_{bq} correction can be used for doses between 500 and 7002 mGy. Using the single-hit model with the single-free-parameter fit to solve for β shows promise in the determination of the intrinsic energy response of film, with β being the mathematical analog of the measured k_{bq} . © 2017 American Association of Physicists in Medicine [https://doi.org/10.1002/mp.12682]

Key words: energy dependence, microdosimetry, radiation dosimetry, radiochromic film, single-hit model

1. INTRODUCTION

Ashland Specialty Ingredients (Bridgewater, NJ) manufactures a variety of radiochromic films, known commercially as GafChromic[®] films, for a range of radiotherapy and diagnostic applications. EBT3 film, the third generation of the External Beam Therapy line, is primarily designed for intensity modulated radiation therapy (IMRT) patient plan verification. Other EBT applications include brachytherapy,^{1,2}

radiobiology,^{3,4} and CT dosimetry,⁵ warranting accurate characterization of EBT response in low-energy and low-dose settings. The latest version of EBT3 contains an active layer that is relatively water equivalent ($Z_{\text{eff}} \approx 7.5$) such that the dose absorbed in its active layer from incident high-energy photons is similar to the dose that would be deposited in an equivalent volume of water. At lower energies, however, the increased cross-sections for photoelectric interactions negate such water equivalence due to the strong dependence of the

photoelectric effect on the atomic number of the high-Z elements within the active layer. This dependence gives rise to an absorbed-dose energy response of EBT3 film that must be taken into account for quantitative radiochromic film dosimetry. The absorbed-dose response for EBT3 can be calculated using analytic or Monte Carlo techniques. Massillon-JL *et al.*⁶ and Brown *et al.*⁷ found contrasting magnitudes of the total energy dependence of EBT3 film to low-energy photons of up to 11% and 3%, respectively. This inconsistency has been attributed to manufacturing and compositional changes that are not always accompanied by updates to the film model or label.^{8–10} Using Monte Carlo simulations of two batches of EBT2 film with slight variations in active layer chemical composition, Sutherland and Rogers¹¹ showed that the magnitude of energy-dependent response for photons under 100 keV is highly dependent on the particular batch makeup (one batch had 10% and the other a 50% energy response). This indicates the necessity for careful determination of the chemical makeup of the active layer for accurate modeling and characterization of the energy response in each film batch. In this work, Monte Carlo methods were used to calculate absorbed-dose energy dependence, f^{rel} , of the latest version of EBT3 film to low-energy x rays.

In addition to absorbed-dose energy dependence, an intrinsic energy response has been reported for most radiochromic film models^{11,12} as well as other solid-state and chemical dosimeters.^{13–18} Intrinsic energy response, denoted k_{bq} , refers to the phenomenon in which different beam energies delivering the same absorbed dose to the film active layer produce different dosimeter responses. These aspects are difficult to model accurately using conventional Monte Carlo codes, and thus, intrinsic energy response is measured or estimated based on empirical data. Previous work¹² has examined these quantities for previous commercially released models and versions of EBT film as well as experimental prototypes. The current work experimentally determines the intrinsic energy response for the current version of EBT3 film through the novel approach of both using the film medium as the reference material, enabling direct measurement of the intrinsic response, as well as using an accompanying mathematical approach to describe the physical processes involved. In addition, a more accurate method for determining intrinsic response by controlling for film's nonlinear response with respect to dose delivered is presented.

Better understanding of the microdosimetric interactions within the active layer of the film can provide the basis for a physical model of intrinsic energy response. Previous work has examined the use of a single-hit geometric model to describe the nonlinear dose-response of EBT film.^{19,20} This work will expand such methodology to investigate how a single-hit model may better quantify the measured intrinsic energy response. The goal of this novel single-hit, microdosimetric model is to account for the polymerization effectiveness of various photon beam qualities. By assuming that the radiochromic response is a result of electronic excitations exceeding the polymerization threshold energy, the complexity of the model is reduced to including only the key features

of the secondary charged particles produced by various photon beam qualities. Thus, this model aims to describe differences in the radiation distributions within active lithium pentacosanoate (LiPCDA) crystals, whose size is on the order of that of mammalian cells,^{21,22} and not the individual excitations of monomeric elements, with sizes of molecular dimensions. Upon successfully quantifying these distribution differences at the crystal level, the single-hit model is used to describe the macroscopic energy response relationships. It is a combination of the microdosimetric model, describing energy distribution throughout a crystal, and the geometric theory, describing the film response given a particular energy distribution, that comprises the proposed film response model.

2. METHODS AND MATERIALS

2.A. Intrinsic energy response

The intrinsic energy response may be written:

$$k_{\text{bq}} = \frac{M_{\text{film}}(Q)}{D_{\text{film}}(Q)}, \quad (1)$$

where a radiation beam with quality Q produces an absorbed dose in film, $D_{\text{film}}(Q)$, and $M_{\text{film}}(Q)$ is the film response measurement (note that this quantity is defined inversely from Sutherland and Rogers,¹¹ Bekerat *et al.*,¹² and Hermida-López *et al.*¹⁰). For direct measurement of the intrinsic energy dependence, the reference beam quality should deliver the same dose to the active film layer as each tested beam quality. The film absorbed-dose energy response in a reference medium is defined as:

$$f(Q) = \frac{D_{\text{med}}(Q)}{D_{\text{film}}(Q)}, \quad (2)$$

where $D_{\text{med}}(Q)$ is the absorbed dose in the reference medium. A reference beam quality, Q_{ref} , which delivers the same dose as the measurement beam quality Q to the medium of interest, may be specified. Then, the relative energy responses, $k_{\text{bq}}^{\text{rel}}(Q)$ and $f_{\text{rel}}(Q)$, may be defined as:

$$k_{\text{bq}}^{\text{rel}}(Q) = \frac{k_{\text{bq}}(Q)}{k_{\text{bq}}(Q_{\text{ref}})} \quad (3)$$

and

$$f_{\text{rel}}(Q) = \frac{f(Q)}{f(Q_{\text{ref}})}. \quad (4)$$

Finally, the total energy dependence of the film, $S(Q)$, may be specified as:

$$S(Q) = \frac{k_{\text{bq}}(Q)}{f(Q)}, \quad (5)$$

and the corresponding relative total energy dependence, $S^{\text{rel}}(Q)$:

$$S^{\text{rel}}(Q) = \frac{k_{\text{bq}}^{\text{rel}}(Q)}{f_{\text{rel}}(Q)}. \quad (6)$$

A key aspect in this work is the use of the film medium itself as the reference material (med) for the determination of the relative intrinsic energy response ($k_{\text{bq}}^{\text{rel}}$). Since D_{film} is determined using Monte Carlo-calculated air kerma-to-dose conversion factors, irradiations were performed by directly relating the x-ray or gamma exposure time to dose to film. Thus, $f^{\text{rel}}(Q)$ was accounted for prior to irradiation for this work, enabling direct measurement of $k_{\text{bq}}^{\text{rel}}(Q)$. To compare with published values and to calculate a relative total energy dependence with respect to water, Monte Carlo simulations were performed using water as the reference material.

This work fully characterizes the energy dependence for ^{60}Co , ^{137}Cs , and a variety of NIST-matched kilovoltage x-ray beam qualities.

2.B. Radiochromic film

To date, there have been three versions of EBT3 radiochromic film produced, with each iteration using a different chemical composition in an effort to make the dosimeter more stable and water equivalent.¹² Two versions of EBT3 film were used for this work, denoted here as version 2 (V2) and version 3 (V3). The original version of EBT3, EBT3-V1, was released in early 2011 and discontinued in October 2011 when EBT3-V2 was initially released. EBT3-V3 was initially released in August 2013, when EBT3-V2 was discontinued. EBT3-V3 is the currently available version of EBT3. All films for each version used in this work were taken from a single lot (A051512-01 and 11051301 for EBT3-V2 and V3, respectively). EBT3-V2 was used in this study for methodology validation and for comparison to previous work, although it is no longer commercially available. The primary difference between EBT3-V2 and EBT3-V3 is the presence and concentration of high-Z materials in the film's active layer, with an increased percentage of aluminum, and the removal of chlorine, sodium, and sulfur in the active layer of EBT3-V3, as shown in Table I. This compositional change is expected to have a negligible effect at photon energies above ^{60}Co ,^{6,9} however, slight changes in the chemical composition can have a major impact (e.g., 50%) on film response to photon energies under 300 keV.¹¹ At low energies, the increase in photoelectric cross-sections is expected to result in a substantial change in dosimeter response, requiring careful quantification of the effect.

Accurate dosimetry with radiochromic film requires consistent and meticulous film handling methods as described by the recommendations of the AAPM Radiation Therapy Task

Group 55.⁸ Latex gloves were worn while handling film to minimize surface contamination. Tweezers and vacuum pickup tools were used for the majority of film handling. To reduce the effects of ambient light,^{24–26} films were stored in opaque envelopes when not in use. Temperature and humidity have been shown to affect film response,^{27–29} so films were stored together in a temperature and humidity-controlled environment to ensure that all films had a similar thermal history, and environmental conditions were documented during irradiation. Storage and irradiation conditions were consistent with manufacturer recommendations. Preirradiation scans were performed at least 48 h after cutting to reduce any effects of the cutting process.³⁰ Postirradiation scans were completed at least 7 days following exposure in order to minimize any changes in the film response due to different postexposure development times.

2.C. Irradiators

The University of Wisconsin Medical Radiation Research Center (UWMRRC) includes a secondary standards laboratory with several irradiators used for this work: a Theratron 1000 ^{60}Co irradiator (Theratron, Inc., Ottawa, ON, Canada), a dual-source G-10 ^{137}Cs irradiator (Hopewell Designs, Inc., Alpharetta, GA, USA), and an (Advanced X-ray, Inc., Buford, GA, USA) constant potential kilovoltage x-ray system. The UWMRRC ^{60}Co irradiator, ^{137}Cs irradiator, and x-ray beams are used as secondary air-kerma standards for the UW Accredited Dosimetry Calibration Laboratory (UWADCL) calibrations of therapy and diagnostic ionization chambers. As secondary standards, the air-kerma rates are directly traceable to NIST and are known to a low uncertainty. The x-ray beams used in this work are matched to lightly filtered (L-series) and moderately filtered (M-series) beams at NIST based on tube voltage, half-value layer (HVL), and homogeneity coefficient (HC). In addition to the L- and M-series beams, a heavily filtered (H-series) 100 kVp beam was also used. The beam qualities used in this work are listed in Table II. Thus, the results of this work offer EBT3 energy characterization for a wide range of beam qualities that are directly traceable to nationally recognized standards.

2.D. Monte Carlo-generated $D_{\text{film}}/K_{\text{air}}$ conversion factors

Monte Carlo simulations were performed using Monte Carlo N-Particle Transport Code (MCNP)³¹ version 6 to

TABLE I. The material compositions of EBT2 and EBT3 film listed in mass percent (%). EBT3 film has undergone three chemical compositions (the first, second, and third versions of EBT3 are denoted here as V1, V2, and V3, respectively), with each iteration becoming more water equivalent.^{12,23}

	H	Li	C	N	O	Na	S	Cl	Br	Al	Z_{eff}	Density (g/cm^3)
EBT2	9.7	0.9	58.4	0.1	28.4	0.4	0.2	1.1	0.8	-	9.38	1.2
EBT3-V1	9.7	0.9	58.4	0.1	28.4	0.4	0.2	1.1	0.8	-	9.38	1.2
EBT3-V2	8.9	1.0	61.3	0.1	23.5	0.5	0.01	4.5	-	0.1	7.99	1.2
EBT3-V3	8.8	0.6	51.1	-	32.8	-	-	-	-	6.7	7.26	1.2

TABLE II. The 15 beam qualities used in this study, with effective energy, first half-value layer, homogeneity coefficient, measured air kerma rates, and Monte Carlo-derived $D_{\text{film}}/K_{\text{air}}$ factors.

UWMRRC beam code	Effective energy (keV)	First HVL (mm Al)	HC	\dot{K}_{air} (mGy/s)	$D_{\text{film}}/K_{\text{air}}$
UW-20M ^a	11.5	0.148	75	1.287	0.919
UW-30M ^a	15.5	0.356	65	1.742	0.959
UW-40M ^a	19.8	0.728	66	1.819	0.977
UW-50M ^a	22.4	1.02	66	2.187	0.983
UW-60M ^a	26.9	1.68	66	1.854	0.993
UW-100L ^a	32.7	2.80	58	3.975	1.008
UW-80M ^a	33.5	2.96	68	1.957	1.006
UW-100M ^a	42.1	4.98	72	1.845	1.022
UW-120M ^a	49.9	6.96	78	2.202	1.036
UW-150M ^a	67.0	10.2	87	2.005	1.054
UW-100H ^b	85.9	13.4	99	0.02377	1.073
UW-200M ^a	99.8	14.9	94	1.654	1.077
UW-250M ^a	145	18.5	98	1.283	1.087
¹³⁷ Cs ^c	662	-	-	0.222	1.128
⁶⁰ Co ^d	1250	-	-	2.764	1.110

^aMoga.³⁴

^bSeelentag *et al.*³⁵

^cSeltzer and Bergstrom.³²

^dMora *et al.*³³

determine the ratio of dose to film per air kerma ($D_{\text{film}}/K_{\text{air}}$) as a function of photon energy for the UWMRRC's ⁶⁰Co, ¹³⁷Cs and NIST-matched kilovoltage x-ray beams. Results of the simulations were used to convert measured air-kerma rates to dose rates to the EBT3-active layer. For the simulations, the ¹³⁷Cs spectrum was taken from the data of Seltzer and Bergstrom,³² and the ⁶⁰Co spectrum was taken from the data of Mora *et al.*³³ The L- and M-series beam spectra used in the MCNP calculations were previously measured using a low-energy germanium detector, corrected with a backward stripping method using Monte Carlo-calculated corrections to account for detector response and other measurement perturbations.³⁴ For the heavily filtered 100 kVp beam (UW100-H), the No. 75 spectrum data from the Gesellschaft für Strahlen-und Umweltforschung mbH München (GSF) Report 560 was used.³⁵ The GSF report contains a compilation of photon spectra data measured with a germanium detector from available institutions. Although not an exact match of the specific beam used in this work, GSF spectra are often assumed to be sufficient for source input used in Monte Carlo simulations.^{13,17,36}

Following the methodology of Davis *et al.*¹³ and Nunn *et al.*¹⁷ for determination of TLD response as a function of photon energy, the $D_{\text{film}}/K_{\text{air}}$ was found using two simulations for each photon beam. The first simulation calculated the energy deposited in the film active layer. The film was modeled within its various configurations of holders (polyethylene vacuum bag, acrylic holder, etc.) as appropriate for the geometry in which the film was irradiated in each beam. The second simulation calculated the air kerma in a volume of air with volume and shape equal to the film active layer.

The film and holders were irradiated free in air, but the Monte Carlo geometry placed the holders in vacuum, since the spectra used in the simulations, aside from the GSF No. 75 beam, are defined at 1 m and corrected for air attenuation. The GSF No. 75 beam is defined at 75 cm, so a (25×25×25) cm³ volume of air was placed between the x-ray point source and the front of the film packet for the UW100-H simulation to correct for the extra attenuation at further distances from the source.

The energy deposition per starting particle was determined using the *F8 tally to calculate the air kerma and the dose deposited in the EBT3 active layer or in an equivalent volume of water for comparison with published work. For the dose simulations, the low-energy electron and photon cutoffs were set to 1 keV. For the simulations of air kerma, electron transport was effectively eliminated by using a low-energy electron cutoff of 2 MeV to force local deposition of energy released in photon interactions. The starting particle direction was sampled from a cone, such that a circular field with diameter of 10 cm was incident on the central depth of the EBT3 active layer. Photons and electrons were transported, and the MCPLIB84 cross-section library³⁷ was used. All materials involved in the simulations (the film active layer, the film polyester substrate layers, the plastic bag, etc.) were modeled as homogeneous mixtures. Dose was defined using energy imparted to the mixture media. A visual rendering, provided by MCNP's Visual Editor (VisEd), of the modeled film for ⁶⁰Co irradiations is shown in Fig. 1.

2.E. Film preparation and preirradiation scanning

A total of three sheets of EBT3-V3 were used to obtain 738 cut and labeled film dosimeters, each measuring (1.2 × 1.2) cm². Similarly, 96 cut and labeled film dosimeters were obtained from one sheet of EBT3-V2 film. The film dosimeters were scanned using the UWMRRC Laser Densitometry System (LDS).³⁸ The LDS is a NIST-traceable laser densitometry system developed in-house that performs point-based measurements of radiochromic film suspended in free-space using coherent light to mitigate common film scanning artifacts, such as positional scan dependence and high noise in low-dose regions.^{39,40} The LDS uses a 635 nm diode laser light source and point photodiode detector. Rosen *et al.*³⁸ demonstrated total elimination of the lateral response artifact (LRA) and minimal nonuniformity using the LDS. Thus, no corrections for LRA or scanner nonuniformity were made. Polarization artifacts due to the coherent light source were also investigated by Rosen *et al.* and were found to be on the order of 0.4% per degree of rotation for 2 Gy exposures. To account for this, care was taken to ensure that films were scanned in the same orientation before and after exposure. Additionally, the uncertainty conservatively assumed maximum response (0.4%/degree) and 1 degree of uncertainty in the film orientation during readout.

Preirradiation optical density (OD) values were determined with the LDS by sequential scanning of each film dosimeter for postirradiation normalization. Following

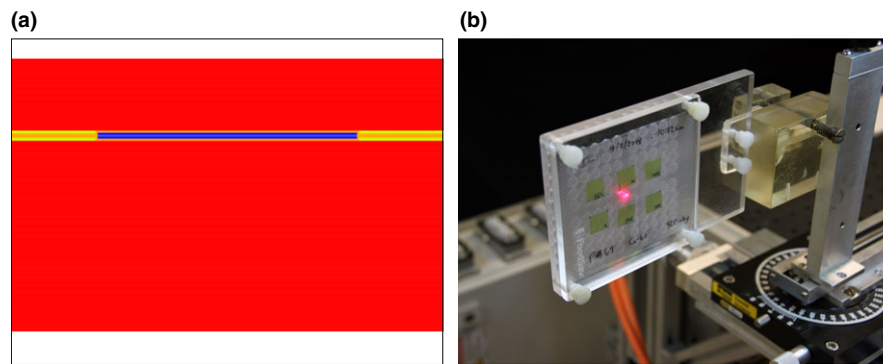


FIG. 1. Geometry of ^{60}Co in-holder simulations and measurements, including (a) a rendering of a film packet in the PMMA holder for simulation in-air with color/material of: white: vacuum, red: PMMA, orange: polyethylene, dark blue: polyester, light blue: active material, green: air and (b) a photograph of a film packet mounted in the PMMA holder for in-air irradiation at one meter from the ADCL ^{60}Co irradiator. Note that for ^{137}Cs and x-ray irradiations, geometries were different with less buildup for ^{137}Cs and no buildup or backscatter material for x rays.

preirradiation scanning, film dosimeters were randomized and placed within thin vacuum-sealed, plastic packets, as described by Rosen,³⁸ Soares,⁴¹ and Massillon-JL *et al.*⁴² The randomization was done in order to minimize the effect of any interfilm (between the three sheets) and intrafilm (within the individual sheet) nonuniformities. Each vacuum-sealed packet contained six film dosimeters as shown in Fig. 2. The vacuum bag was included in the Monte Carlo models as polyethylene, with chemical formula $(\text{C}_2\text{H}_4)_n$ assumed.⁴³ The average bag thickness was determined to be $0.10 \text{ mm} \pm 0.03 \text{ mm}$, using digital caliper measurements of various vacuum bags, while the nominal film thickness, according to the manufacturer, is 0.275 mm . With small thicknesses relative to the overall film thickness and overall setup reproducibility of $\pm 1 \text{ mm}$, the added uncertainty was

minimal. The maximum Monte Carlo calculated variation from the intended dose due to the bags was found to be well under 1%, even at the lower energies.

2.F. Film irradiations

For film irradiation with x rays, multiple pieces of Kapton[®] tape were used to suspend the film packets in air from a polymethyl-methacrylate (PMMA) fixture with an opening of $(15.5 \times 13.5) \text{ cm}^2$. The Kapton tape was used to suspend the packets in air away from the PMMA fixture in order to minimize scatter while simultaneously positioning the dosimeter packets normal to the x-ray beam. Figure 2 shows photographs of this setup for the x-ray irradiations. For ^{137}Cs and ^{60}Co irradiations, the dosimeter packets were placed in an

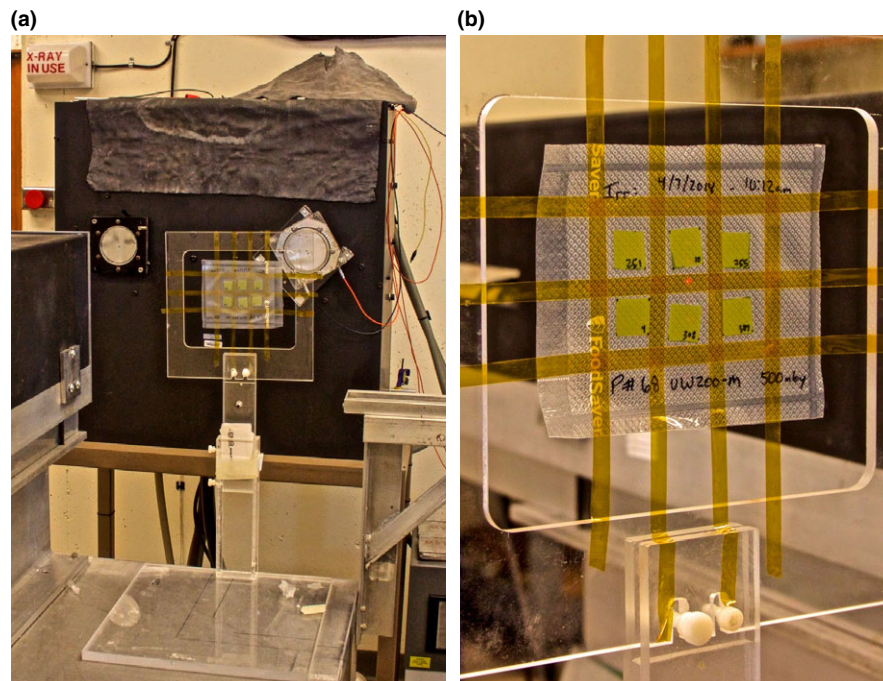


FIG. 2. Photographs of the film irradiation geometry for x-ray energies. [Color figure can be viewed at wileyonlinelibrary.com]

acrylic phantom holder in order to obtain appropriate buildup and backscatter. This holder had a (10×10) cm² face, with a back plate thickness of 8.8 mm. A 5.2-mm thick front plate was used for the ⁶⁰Co irradiations, and a 2.9-mm thick plate was used for the ¹³⁷Cs irradiations in order to achieve charged particle equilibrium as described by Nunn *et al.*¹⁷ The holders were modeled in MCNP to account for any scatter dose or spectral changes caused by the presence of the holder material. Films positioned within the PMMA holder for ⁶⁰Co irradiations are shown in Fig. 1.

Seven film dosimeter packets were exposed to seven different dose levels for each energy. The delivered doses to the film active layers were: 57, 103, 500, 699, 997, 1998, and 7002 mGy. Dose rates for each beam were determined based on the air-kerma rates measured using a NIST-calibrated UWADCL secondary standard ionization chamber and the Monte Carlo-determined $D_{\text{film}}/K_{\text{air}}$ conversion factors.

2.G. Film postirradiation scanning

For all postirradiation analyses, film samples were scanned at least seven days following exposure to minimize change in film response due to small variations in development duration.^{44,45} Film was scanned postirradiation in the same numerical order as it was scanned prior to irradiation to mitigate any positional or temporal nonuniformities associated with the LDS scanner.³⁸ In order to provide a calibrated optical density measurement, a series of NIST-traceable calibrated reference materials (CRMs) bracketing the expected film OD range were included with every scan. The CRMs used were Kodak WrattenTM 2 No. 96 Polyester Neutral Density Filters. OD was determined by applying a linear fit between the NIST-provided reference OD and the LDS-measured OD for each CRM.

2.H. Data analysis

Film response was taken as the difference between net optical densities of exposed dosimeters and unirradiated controls (Δ_{netOD}). Since packets received the same dose to film across all beam qualities, differences in response between energies are due to intrinsic EBT3 energy dependence. Normalized intrinsic EBT3 energy dependence was found by taking the ratio of response for a given beam quality to the response when exposed to ⁶⁰Co. The results were compared with recently published data using similar techniques.¹²

2.I. Single-hit theory

Understanding the measured intrinsic response requires an examination into the microdosimetric interactions within the active layer of the EBT3 film. The active layer consists of two main components: the diacetylene monomer LiPCDA crystals (the active component), and the gelatin in which they are suspended. The LiPCDA crystals are stick-like monomer crystals of varied lengths and widths. These crystals are densely arranged throughout the active layer.⁴⁶ Callens *et al.*²⁰

found that there is a wide range of sizes of the crystals, with a mean length of 9.4 ± 5.6 μm and a mean width of 1.62 ± 0.35 μm .

Lineal energy transfer is the energy transferred from a particle to the medium traversed per unit length, and is the microdosimetric analog to Linear Energy Transfer (LET). The mean lineal energy deposition changes with energy. The lower the energy, the lower the deposition range as determined by the continuous slowing down approximation (CSDA). At lower energies, this reduced deposition range results in more energy deposited in a smaller area of the active layer relative to higher energies and their wider, more spread out, deposition. It is hypothesized that the higher energies reach more active centers than the lower energies. As discussed earlier, each successive compositional change in the active layer has led to more water equivalence and an expected decrease of the overall energy dependence. Understanding how the composition of the active layer affects the microdosimetric interactions between the incoming radiation and the active LiPCDA crystals is essential for estimating the intrinsic energy response of the film.

For this work, a simplified model of the polymerization mechanics in the EBT3 film is used. This model aims to describe differences in the radiation distributions within active LiPCDA crystals and not the individual, molecular-level excitations of monomeric elements. This work makes some assumptions. The first assumption is that the LiPCDA crystals are either “on” or “off”: “on” if radiation has hit its active center, and “off” if it has not. The second assumption is that there is a probability that a threshold amount of radiation will activate a center, and that there are a finite number of crystals in any given area of the film active layer. Since the threshold energy required to induce polymerization is on the order of a single eV,⁴⁷ the accumulation of energy below this threshold can be largely ignored when ionizing radiation is considered. Instead, the ionization density relative to the active center spacing is considered to be the driver of intrinsic response differences. Finally, if radiation is present but no “off” crystals are available for interaction, saturation occurs. Thus, for lower energies, shorter deposition ranges result in higher radiation density in a smaller area and fewer available active centers to interact with. This leads to saturation at relatively lower doses as compared to higher energies.

From the single-hit model discussed in del Moral *et al.*,¹⁹ the number of active centers struck (m) is related to the total number of active centers per unit area (M) using the equation:

$$m = M(1 - e^{-\Phi\sigma}), \quad (7)$$

where Φ is the planar fluence of directly ionizing radiation, and σ is the cross-section of interaction between active centers and radiation. If we assume charged-particle equilibrium (which is present in the experimental setups in this work), Φ is proportional to dose (D) using the equation:

$$\Phi = \beta D. \quad (8)$$

The hypothesis is that the proportionality constant, β , is dependent on beam quality, Q ; such that the secondary

electron fluence within active centers depends on Q , but the cross-section of interaction, σ , is proportional only to the size of the active centers. For the simple model, we assume that the mean size of the active centers is the size of all active centers (which is a film invariant). σ is the constant cross-section of interaction (which can be thought of as the physical, geometric cross-section of the centers). Since optical density for a given quality Q is proportional to m , the following relationship can be written:

$$OD_Q \propto M(1 - e^{\beta_Q D_Q \sigma}). \quad (9)$$

By including a proportionality constant, α , which represents the scanner response per hit active center, the following fit function can be applied for each beam quality:

$$OD_Q = \alpha M(1 - e^{\beta_Q D_Q \sigma}), \quad (10)$$

where α is considered a LDS scanner constant, while M and σ are considered to be EBT3 film constants.

For the 15 beam qualities and seven dose levels described previously, OD values were determined using the described methodology. Then, a four-parameter fit function [Eq. (10)] was applied only to the reference beam quality (^{60}Co), to determine the scanner and film constants, α , M , and σ . For the remaining 14 beam qualities, the model predicts that the single free parameter, β_Q , fully characterizes the intrinsic energy dependence and may be determined by fixing the remaining three parameters to match those determined using the reference beam. Once β_Q is determined for all beam qualities, the following equation is applied:

$$\beta_Q / \beta_{\text{ref}} = \beta_{\text{rel}}, \quad (11)$$

where β_{rel} is the relative relationship of the beam quality of interest to ^{60}Co . Once validated, this methodology may provide users with a straightforward way to characterize intrinsic energy dependence in arbitrary beam qualities.

3. RESULTS

3.A. Intrinsic energy and dose dependence

The intrinsic, absorbed-dose, and total energy responses of EBT3-V3 film relative to ^{60}Co are included in Table III. The measured intrinsic energy response for dose levels 500 mGy and greater are plotted in Fig. 3. Under-response to low energies, as well as a dip in response at approximately 67 keV, are relatively consistent across all five dose levels as noticeable in Fig. 3. For effective energies of 19 to 145 keV, the intrinsic energy response is relatively consistent, ranging from 3% to 7% under-response relative to ^{60}Co . The maximum standard deviation of the mean of the five dose levels for all energies was 2.2%. All dose differences were within the overall uncertainty of the measurements (3.65% at the $k = 2$ level). For further uncertainty discussion, see the Uncertainty Analysis section below. It is of note that using different reference media has the potential to result in different $k_{\text{bq}}^{\text{rel}}$ values due to differences in total dose to the film active layer. While this work has shown minimal dose

TABLE III. Measured intrinsic, calculated absorbed-dose, and total energy response of EBT3-V3 relative to ^{60}Co for dose levels 500–7002 mGy. Uncertainty for the intrinsic energy response results are displayed as the standard deviation of the mean response over all doses at a given effective energy. The absorbed-dose uncertainties are the propagated statistical errors of the Monte Carlo $D_{\text{film}}/K_{\text{air}}$ calculations.

Effective energy (keV)	UWMRRC beam quality	Intrinsic ($k_{\text{bq}}^{\text{rel}}$)	Absorbed dose ($1/f_{\text{ADW}}^{\text{rel}}$)	Total ($S^{\text{rel}} = k_{\text{bq}}^{\text{rel}}/f^{\text{rel}}$)
11.5	UW-20M	0.822 ± 1.9%	0.988 ± 0.3%	0.812 ± 1.9%
15.5	UW-30M	0.898 ± 1.6%	0.977 ± 0.4%	0.877 ± 1.6%
19.8	UW-40M	0.934 ± 2.1%	0.974 ± 0.4%	0.910 ± 2.1%
22.4	UW-50M	0.954 ± 1.6%	0.972 ± 0.5%	0.928 ± 1.7%
26.9	UW-60M	0.973 ± 2.2%	0.965 ± 0.6%	0.939 ± 2.3%
32.7	UW-100L	0.957 ± 1.5%	0.960 ± 0.7%	0.918 ± 1.6%
33.5	UW-80M	0.958 ± 1.2%	0.956 ± 0.8%	0.916 ± 1.4%
42.1	UW-100M	0.959 ± 1.9%	0.954 ± 0.8%	0.915 ± 2.1%
49.9	UW-120M	0.941 ± 1.2%	0.946 ± 0.8%	0.890 ± 1.5%
67.0	UW-150M	0.934 ± 0.9%	0.950 ± 0.7%	0.887 ± 1.1%
85.9	UW-100H	0.947 ± 0.8%	0.960 ± 0.7%	0.909 ± 1.1%
99.8	UW-200M	0.947 ± 2.2%	0.971 ± 0.7%	0.920 ± 2.3%
145	UW-250M	0.966 ± 2.1%	0.993 ± 0.8%	0.959 ± 2.3%
662	^{137}Cs	1.000 ± 1.8%	1.009 ± 0.4%	1.009 ± 1.9%

dependence for the intrinsic energy response, it is worth consideration when using different reference media.

The values for the two lowest dose levels, 57 and 103 mGy, were not included in Table III or Fig. 3 due to poor signal resulting in high statistical uncertainty. This signal-to-noise issue is exacerbated at the lower energies, at which the intrinsic under-response is greatest. Due to the high uncertainty, it is unclear whether doses lower than 500 mGy exhibit similar intrinsic energy response as higher doses. The dynamic range of the EBT3/LDS dosimetry system is determined by the signal-to-noise (SNR) ratio at a variety of dose levels. In this application, SNR was reduced by a factor of 3 and 2.5 for dose levels of 57 and 103 mGy, respectively, as

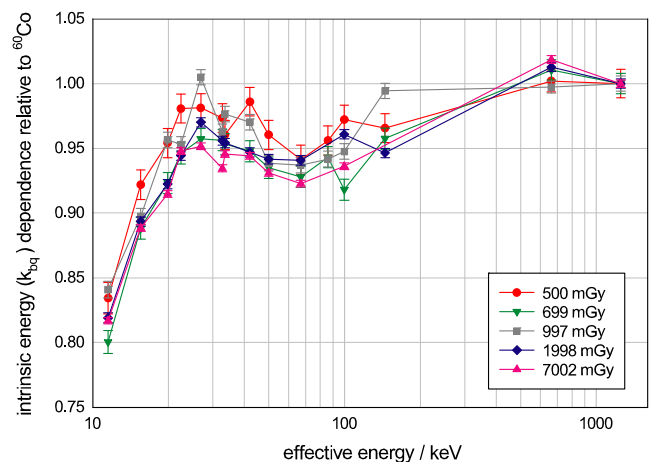


FIG. 3. Intrinsic energy response of GafChromic EBT3-V3 film by dose level. Error bars are the standard deviation of the mean for the six individual film OD readings. [Color figure can be viewed at wileyonlinelibrary.com]

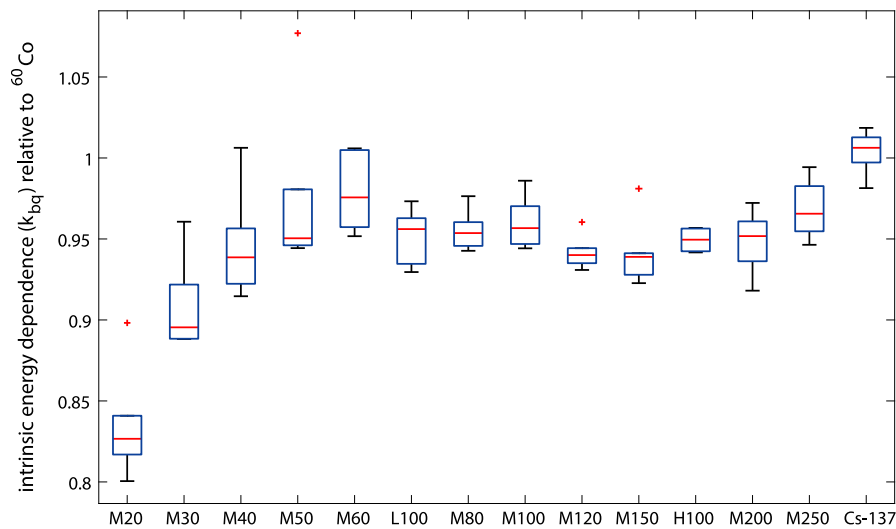


FIG. 4. The spread and skewness of the intrinsic energy dependence normalized to ^{60}Co is shown for each measured beam, with the 103 mGy dose level included. The central line inside the box for each beam represents the median of the data, and the upper and lower limits of the box represent the 75th and 25th percentiles, respectively. Data outside of three times the interquartile range were considered outliers, and are plotted individually as dots. The whiskers indicate the upper and lower limits of dataset, not including any outliers. Note that all outliers are 103 mGy values. [Color figure can be viewed at wileyonlinelibrary.com]

compared to 1998 mGy. Since up to an additional 20% response reduction for EBT3-V3 is evident for the lowest-energy beam qualities, noise limitations prevented an accurate characterization of energy response at these two dose levels.

Figure 4 shows the distribution of the intrinsic response over all dose levels between 103 and 7002 mGy. The 103 mGy dose level was added to this analysis to demonstrate the issues of low-energy, low-dose relative measurements. Including the 103 mGy data increases the standard deviation for all energies, and also greatly increases the deviation from ^{60}Co response at lower energies. The limited signal at low energies (due to under-response) at low dose levels prevents meaningful interpretation of experimental data that was attained at both low energy and low dose levels.

3.B. Measurement uncertainty analysis

A full uncertainty analysis for the results of this work is shown in Table IV. The analysis was completed in accordance with the NIST Technical Note 1297 methodology.⁴⁸ The air-kerma and beam uniformity uncertainties were taken from the UWADCL uncertainty budgets for therapy-class ion chamber calibrations.⁴⁹ The film positioning uncertainty includes both the repeatability of the film placement within the alignment systems as well as the precision of the alignment systems. This positioning uncertainty is based on a precision of ± 1 mm, and a rectangular distribution was assumed. The film and scanner uniformity uncertainty includes both inter- and intrafilm uncertainty as well as the LDS measurement uncertainty. The Type A contribution to this uncertainty value is based upon the average standard deviation of the measured OD for every pack of six films (70 of these packs total) while the Type B contribution is based upon the highest standard deviation for any one of these

packs. The highest standard deviation was used to establish an upper limit on the uncertainty, and a rectangular distribution was assumed. The additional film development uncertainty is the added uncertainty in the film development due to variables not directly related to the irradiation of the film as investigated in previous versions of EBT film. Exposure to UV light,^{24–26} temperature and humidity fluctuations during storage and scanning,^{27–29} and differences in the postexposure delay before scanning^{44,45} can all contribute to unwanted, varied film development if not controlled. As discussed in the Methods section, great care was taken to follow past recommendations for other formulations of EBT film and minimize these effects. As many of these past investigations were on previous versions of EBT film, a cautious approach in estimating the uncertainty due to these variables was taken. The value of 0.5% is both a reflection of the potential added uncertainty found in these studies as well as internal measurements based on our methodology and our formulation of the EBT3 film. The scan orientation uncertainty is a conservative estimate based upon the LDS rotational dependence study as described in Rosen *et al.*³⁸ The study found that the potential rotational variance possible for a piece of film within the LDS holder was negligible. The Monte Carlo uncertainties account for uncertainties in the calculation of the ratios of dose to film per air kerma ($D_{\text{film}}/K_{\text{air}}$) that were used to determine the dose delivered to each set of films. Uncertainty due to inexact spectra is expected to be minimal as two beams with similar effective energies but different spectra, UW-100L and UW-80M, have similar relative energy response. Per Nunn *et al.*,¹⁷ the largest contribution to this uncertainty was the impact of low-energy photons. Simulations were performed using photon energy cutoffs of both 1 and 10 keV to determine the potential effect on the various beam qualities. As expected, the change in photon cutoff energy primarily affected the lower energy

TABLE IV. Uncertainty budget for the intrinsic energy response (k_{bq}) determination. Film irradiation, scanning, as well as MC calculated $D_{\text{film}}/K_{\text{air}}$ ratio uncertainties are included.

Parameter	Type A	Type B
<i>Irradiation</i>		
^{60}Co air-kerma rate determination		0.73
^{137}Cs air-kerma rate determination		0.78
X-ray air-kerma rate determination		0.45
Beam uniformity		0.10
Film positioning		0.12
<i>Measurement</i>		
Film and scanner uniformity	0.45	0.55
Additional film development		0.50
Scan orientation		0.40
<i>Monte Carlo Calculations</i>		
Statistical computational uncertainty	0.20	
Energy cutoff		0.07
Photon spectrum		0.50
Cross sections		0.86
Quadratic sum	0.49	1.76
A and B quadratic sum		1.82
Total combined uncertainty		1.82 ($k=1$)
Expanded total uncertainty		3.65 ($k=2$)

beams. Percent change between the two simulations was determined for each beam quality and a rectangular distribution was assumed.

3.C. Single-hit results

Table V shows the results of the single-free-parameter (β) fit calculations derived from the single-hit model in this work. To compare these results with the intrinsic energy data, β_{rel} and $k_{\text{bq}}^{\text{rel}}$ are listed and compared. The correlation between β_{rel} and $k_{\text{bq}}^{\text{rel}}$ suggests that β , at least in part, characterizes the microdosimetric interactions that determine the intrinsic energy response of the film and that β_Q is indeed a description of the fluence per unit dose in the active centers.

3.D. EBT3-V2 and EBT3-V3 comparison

Figure 5 shows a comparison of the measured intrinsic energy response of both EBT3-V2 and EBT3-V3 at 699 mGy. Note that the compositional change in V3 has greatly improved the low-energy under-response evident in V2. This improvement in response is of interest as it represents the change in energy deposition within the film active layer between the two formulations. As discussed earlier, lower energies have a lower deposition range relative to higher energies, and the higher Z elements in the active layer of the EBT3-V2 further increase the attenuation properties of the active layer gelatin. This leads to a decreased deposition range and, therefore, fewer active centers available for interaction with incoming radiation, exacerbating the saturation issue for low energies. Conversely, the more water equivalent

TABLE V. β fitting parameters and β^{rel} values compared with $k_{\text{bq}}^{\text{rel}}$.

Beam quality	Effective energy (keV)	Beta (β) ($\times 10^{-4}$)	Chi-squared fit statistic ($\times 10^{-3}$)	β^{rel}	$k_{\text{bq}}^{\text{rel}}$	$\beta^{\text{rel}}/k_{\text{bq}}^{\text{rel}}$
UW-20M ^a	11.5	1.225	0.957	0.763	0.822	0.928
UW-30M ^a	15.5	1.369	0.853	0.853	0.898	0.950
UW-40M ^a	19.8	1.427	1.065	0.889	0.934	0.952
UW-50M ^a	22.4	1.491	1.698	0.929	0.954	0.974
UW-60M ^a	26.9	1.510	0.765	0.941	0.973	0.967
UW-100L ^a	32.7	1.473	0.675	0.918	0.957	0.959
UW-80M ^a	33.5	1.492	0.948	0.930	0.958	0.970
UW-100M ^a	42.1	1.487	1.305	0.927	0.959	0.966
UW-120M ^a	49.9	1.459	0.843	0.909	0.941	0.966
UW-150M ^a	67.0	1.444	0.451	0.900	0.934	0.964
UW-100H ^b	85.9	1.462	0.239	0.911	0.947	0.962
UW-200M ^a	99.8	1.474	0.490	0.918	0.947	0.970
UW-250M ^c	145	1.453	1.411	0.905	0.966	0.937
$^{137}\text{Cs}^{\text{a}}$	662	1.642	5.069	1.023	1.008	1.015
$^{60}\text{Co}^{\text{a}}$	1250	1.605	3.030	1.000	1.000	1.000

^aOD values for all five doses used.

^bOD values for doses 500, 699, and 997 mGy used (1997 and 7002 mGy irradiations were not performed due to irradiation time restraints).

^cOD values for doses 500, 699, 997, and 1997 mGy used (7002 mGy not used due to irradiation error).

(lower Z) EBT3-V3 film allows for a wider deposition range resulting in less saturation.

4. DISCUSSION

Table III shows the measured intrinsic, calculated absorbed-dose, and combined total energy response of EBT3-V3 film. A sample uncertainty budget is included in Table IV. Since the spread of the measured intrinsic energy response results are taken as an estimate of the uncertainty

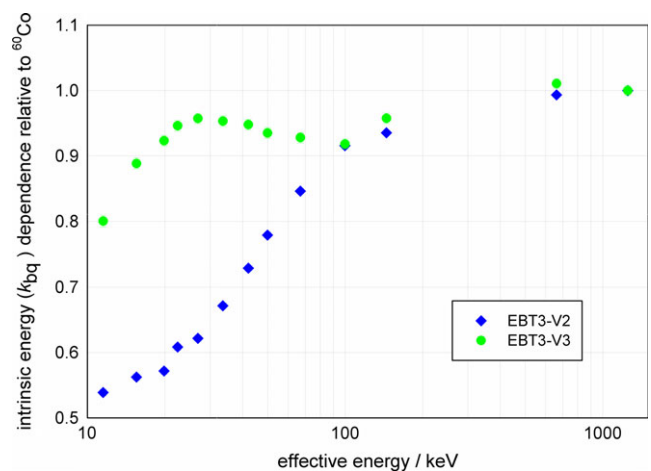


Fig. 5. The intrinsic energy response relative to ^{60}Co at 699 mGy for EBT3-V2 and EBT3-V3. Error bars are the standard deviation of the mean for the individual film OD readings and are included but mostly obscured by data point markers. [Color figure can be viewed at wileyonlinelibrary.com]

for the intrinsic energy response, the standard deviation of the mean response over all doses at a given effective energy was added in quadrature with the Monte Carlo-calculated statistical uncertainty to calculate Type A uncertainty. Tabulated Type B uncertainties are listed in Table IV.

4.A. Application of intrinsic energy-response correction

The intrinsic energy responses listed in Table III can be used to normalize the response of EBT3-V3 films irradiated at two or more different energies. These correction factors are applicable for doses between 500 and 7002 mGy.

EBT3-V3 film has a greatly reduced energy dependence as compared to previous iterations of EBT films;^{11,12} however, this energy dependence still warrants consideration at lower energies. When performing comparative quantitative analysis between film samples in different irradiation environments or geometries, it is necessary to know the effective energy or energies of incoming radiation at the active layer of film, which requires an understanding of the initial radiation spectrum and spectral changes throughout the media. In most cases (i.e., other than “in-air” irradiations), Monte Carlo simulations are required to calculate the spectrum and effective energy of the beam at the film’s active layer accurately.

To reduce measurement uncertainties, matching the effective energy between measurement and calibration films is optimal; however, this is often not possible due to differences in irradiation geometry, which are especially important at lower energies. In these situations, applying intrinsic (k_{bq}) and absorbed-dose (f^{rel}) energy corrections is likely the next-best alternative. For effective energies not listed in Table III, one could use the methodology described in this paper to obtain specific correction factors. Another less certain (although more practical) option would be to match the experimental effective energy using nearest neighbor or spline interpolation.

As discussed earlier, manufacturing and compositional changes of EBT3 film have not always been accompanied by updates of the film model or label. As seen when comparing EBT3-V2 and EBT3-V3 film, any compositional change in the active layer of the film can result in substantial change in the energy response of the film. Because of this, it is recommended that the composition of any new batch of film be verified when multiple effective energies are involved. This can be achieved through literature review, contacting the manufacturer, or performing energy calibration checks following the methodology presented in this manuscript.

4.B. Comparison with previous work

The EBT3-V3 total energy response relative to ^{60}Co derived in this work and that from Bekerat *et al.*¹² is plotted in Fig. 6. It is noted that while the effective energy values of the beams in the two compared studies are similar, the spectra of the beams are not identical. Nevertheless, the similarity of the results for UW-100L, the minimally filtered 100 kVp

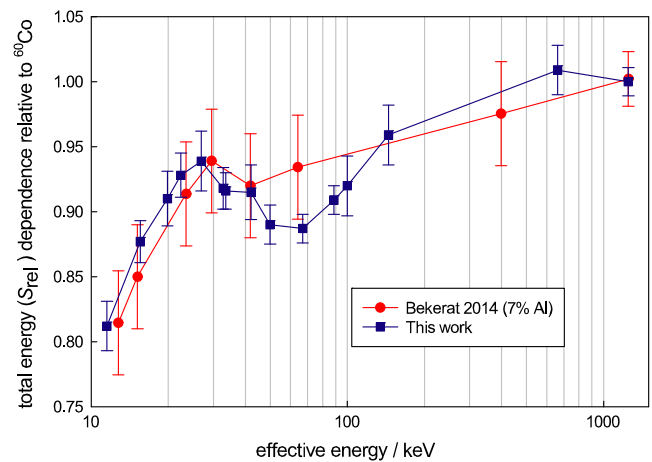


Fig. 6. Comparison of the results of the total energy response relative to ^{60}Co for EBT3-V3 from this work to those of Bekerat *et al.*¹² for similar beams. Note that both sets of film feature the compositional improvement of substituting the Cl and Br of past EBT3 iterations for 7% Al. Error bars for the current work represent uncertainty from intrinsic and absorbed-dose uncertainties added in quadrature (summarized in Table IV), while error bars for Bekerat *et al.* represent the stated and plotted deviations listed in the published work. [Color figure can be viewed at wileyonlinelibrary.com]

beam, and those for UW-80M, the moderately filtered 80 kVp beam (two beams with similar effective energies but different spectra) indicate that small changes in spectra may not have a large effect on results. It should also be noted that different dose to film was delivered in this work and any potential dose dependence of the intrinsic response may affect the comparison. However, in this work we have shown minimal intrinsic response dose dependence in the range of doses investigated.

Comparison with Bekerat *et al.* indicates that, although methodologies were different, the results of this work are consistent with previously published values within reported uncertainties. It is likely that the lower overall measurement uncertainty reported in this work is a result of (a) the use of a measurement light source tuned to match the EBT3 absorption spectrum³⁸ and (b) the use of direct measurement of intrinsic energy response by essentially eliminating the absorbed-dose component of the energy response.

4.C. Single-hit discussion

The correlation between β_{rel} and $k_{\text{bq}}^{\text{rel}}$ suggests that β partially characterizes the microdosimetric interactions that determine the measured intrinsic energy response of the film, and that the proportionality constant, β_Q , is indeed a description of the amount of fluence per unit dose in the active centers for a particular beam quality. The results support the hypothesis that higher energies are able to interact with more active centers relative to lower energies, and that saturation due to a more limited number of active centers per unit of radiation is an underlying cause of the film under-response at lower energies.

It is likely that more advanced fitting models, such as percolation theory as discussed by del Moral *et al.*¹⁹ will

continue to refine and improve the β -fitting process. With the individual microdosimetric parameters defined, successful modeling of the intrinsic energy response through Monte Carlo computations may be feasible. The measured results of this work provide a means for benchmarking future refinements to the microdosimetric understanding of radiochromic film response.

5. CONCLUSION

This study has determined the intrinsic energy response for EBT3-V3 GafChromic radiochromic film. The k_{bq} correction factors are listed in Table III for direct comparison of films irradiated at different energies. The variation in these k_{bq} factors demonstrates the need to correct for differences in effective energies used in any such comparison. Use of the measured intrinsic energy response, along with the calculated absorbed-dose energy response, can greatly reduce the measurement uncertainties for film irradiations involving multiple energies. Further investigation into mitigating low dose (< 500 mGy) signal effects on measuring intrinsic energy is also warranted.

Using the single-hit model with the single-free-parameter fit to solve for β shows promise in the determination of the intrinsic energy response of film, with β being the mathematical analog of the measured k_{bq} . Further refinement of the calculation of β through more advanced modeling, such as percolation theory or detailed Monte Carlo simulation, has the potential to provide an accurate theoretical estimation of EBT3 film intrinsic energy response.

ACKNOWLEDGMENTS

The authors thank Dr. David Lewis, formerly of Ashland Specialty Ingredients (Bridgewater, NJ), for providing the EBT3 films used in this work. The authors also thank the University of Wisconsin Radiation Calibration Laboratory (UWRCL) and the University of Wisconsin Accredited Dosimetry Calibration Laboratory (UWADCL) customers, whose calibrations help support ongoing research at the UWMRRC.

CONFLICTS OF INTEREST

The authors have no relevant conflicts of interest to disclose.

^{a)} Author to whom correspondence should be addressed. Electronic mail: cghammer@wisc.edu.

REFERENCES

- Chiu-Tsao S-T, Medich D, Munro J, III. The use of new GAFCHROMIC[®] EBT film for ¹²⁵I seed dosimetry in Solid Water[®] phantom. *Med Phys*. 2008;35:3787–3799.
- Palmer AL, Lee C, Ratcliffe AJ, Bradley D, Nisbet A. Design and implementation of a film dosimetry audit tool for comparison of planned and delivered dose distributions in high dose rate (HDR) brachytherapy. *Phys Med Biol*. 2013;58:6623–6640.
- Wong J, Armour E, Kazanzides P, et al. High-resolution, small animal radiation research platform with x-ray tomographic guidance capabilities. *Int J Radiat Oncol Biol Phys*. 2008;71:1591–1599.
- Fowler TL, Fulkerson RK, Micka JA, Kimple RJ, Bednarz BP. A novel high-throughput irradiator for in vitro radiation sensitivity bioassays. *Phys Med Biol*. 2014;59:1459.
- Gotanda R, Katsuda T, Gotanda T, Tabuchi A, Yatake H, Takeda Y. Dose distribution in pediatric CT head examination using a new phantom with radiochromic film. *Australas Phys Eng Sci Med*. 2008;31:339–44.
- Massillon-JL G, Chiu-Tsao S, Domingo-Munoz I, Chan M. Energy dependence of the new gafchromic EBT3 film: dose response curves for 50 kV, 6 and 15 MV x-ray beams. *Int J Med Phys Clin Eng Radiat Oncol*. 2012;1:60–65.
- Brown TA, Hogstrom KR, Alvarez D, Matthews KL, II, Ham K, Dugas JP. Dose-response curve of EBT, EBT2, and EBT3 radiochromic films to synchrotron-produced monochromatic x-ray beams. *Med Phys*. 2012;39:7412–7417.
- Niroomand-Rad A, Blackwell CR, Coursey BM, et al. Radiochromic film dosimetry: recommendations of AAPM Radiation Therapy Committee Task Group 55. *Med Phys*. 1998;25:2093–2115.
- Villarreal-Barajas JE, Khan RFH. Energy response of EBT3 radiochromic films: implications for dosimetry in kilovoltage range. *J Appl Clin Med Phys*. 2014;15:331–338.
- Hermida-López M, Lüdemann L, Flühs A, Brualla L. Technical note: influence of the phantom material on the absorbed-dose energy dependence of the EBT3 radiochromic film for photons in the energy range 3 keV–18 MeV. *Med Phys*. 2014;41:112103-1–112103-6.
- Sutherland JGH, Rogers DWO. Monte Carlo calculated absorbed-dose energy dependence of EBT and EBT2 film. *Med Phys*. 2010;37:1110–1116.
- Bekerat H, Devic S, DeBlois F, et al. Improving the energy response of external beam therapy (EBT) GafChromicTM dosimetry films at low energies (≤ 100 keV). *Med Phys*. 2014;41:022101-1–022101-14.
- Davis SD, Ross CK, Mobit PN, Van der Zwan L, Chase WJ, Shortt KR. The response of LiF thermoluminescence dosimeters to photon beams in the energy range from 30 kV x rays to ⁶⁰Co gamma rays. *Radiat Prot Dosim*. 2003;106:33–43.
- Santos AMC, Mohammadi M, Afshar SA. Energy dependency of a water-equivalent fibre-coupled beryllium oxide (BeO) dosimetry system. *Rad Meas*. 2015;73:1–6.
- Anton M, Büermann L. Relative response of the alanine dosimeter to medium energy x-rays. *Phys Med Biol*. 2015;60:6113–6129.
- Reed JL, Rasmussen BE, Davis SD, Micka JA, Culberson WS, DeWerd LA. Determination of the intrinsic energy dependence of LiF:Mg,Ti thermoluminescent dosimeters for ¹²⁵I and ¹⁰³Pd brachytherapy sources relative to ⁶⁰Co. *Med Phys*. 2014;41:122103-1–122103-11.
- Nunn AA, Davis SD, Micka JA, DeWerd LA. LiF:Mg,Ti, TLD response as a function of photon energy for moderately filtered x-ray spectra in the range of 20 to 250 kVp relative to ⁶⁰Co. *Med Phys*. 2008;35:1859–1869.
- Olko P, Bilski P, Kim JL. Microdosimetric Interpretation of the Photon Energy Response of LiF:Mg,Ti Detectors. *Radiat Prot Dosim*. 2002;100:119–122.
- del Moral F, Vázquez JA, Ferrero JJ, et al. From the limits of the classical model of sensitometric curves to a realistic model based on the percolation theory for GafchromicTM EBT films. *Med Phys*. 2009;36:4015–4026.
- Callens MB, Crijns W, Depuydt T, et al. Modeling the dose dependence of the vis-absorption spectrum of EBT3 Gafchromic[®]. *Med Phys*. 2017;44:2532–2543.
- Rink A, Jaffray DA. Fiber optic-based radiochromic dosimetry. In: S. Beddar, L. Beaulieu, eds. *Scintillation Dosimetry*. New York, NY: CRC Press; 2016:293–314.
- Saladin KA. *Human Anatomy*. Madison, WI: McGraw Hill; 2005.
- Rosen BS. 2015. Advanced radiochromic film methodologies for quantitative dosimetry of small and nonstandard fields. Ph.D. thesis, University of Wisconsin, Madison, WI.
- Andrés C, del Castillo A, Tortosa R, Alonso D, Barquero R. A comprehensive study of the GafChromic EBT2 radiochromic film. A comparison with EBT. *Med Phys*. 2010;37:6271–6278.

25. Butson MJ, Yu PKN, Metcalfe PE. Effects of read-out light sources and ambient light on radiochromic film. *Phys Med Biol*. 1998;43:2407–2412.
26. Butson MJ, Yu PKN, Cheung T, Metcalfe PE. Radiochromic film for medical radiation dosimetry. *Mat Sci Eng R*. 2003;41:61–120.
27. Lynch BD, Kozelba J, Ranade MK, Li JG, Simon WE, Dempsey JF. Important considerations for radiochromic film dosimetry with flatbed CCD scanners and EBT GAFCHROMIC[®] film. *Med Phys*. 2006;33:4551–4556.
28. Rink A, Lewis DF, Varma S, Vitkin IA, Jaffray DA. Temperature and hydration effects on absorbance spectra and radiation sensitivity of a radiochromic medium. *Med Phys*. 2008;35:4545–4555.
29. Girard F, Bouchard H, Lacroix F. Reference dosimetry using radiochromic film. *J Appl Clin Med Phys*. 2012;13:339–353.
30. Klassen NV, van der Zwan L, Cygler J. Gafchromic MD-55: investigated as a precision dosimeter. *Med Phys*. 1997;24:1924–1934.
31. X-6 Monte Carlo Team. MCNP6 users manual - code version 6.1.1beta, Report LA-CP-14-00745. Los Alamos National Laboratory, Los Alamos, NM, 2014.
32. Seltzer SM, Bergstrom PM. Changes in the U.S. primary standard for the air-kerma from gamma-ray beams. *J Res Natl Inst Stand Technol*. 2003;108:359–381.
33. Mora GM, Maio A, Rogers DWO. Monte Carlo simulation of a typical ⁶⁰Co therapy source. *Med Phys*. 1999;26:2494–2502.
34. Moga JD. Characterization of low-energy photon-emitting brachytherapy sources and kilovoltage x-ray beams using spectrometry. Ph.D. dissertation, UW-Madison, 2011.
35. Seelentag WW, Panzer W, Drexler G, Platz L, Santer F. A catalogue of spectra used for the calibration of doseimeters. Tech. Rep. 560, Gesellschaft für Strahlen- und Umweltforschung mbH, Munchen, 1979.
36. McCabe BP, Speidel MA, Pike TL, Van Lysel MS. Calibration of Gafchromic XR-RV3 radiochromic film for skin dose measurement using standardized x-ray spectra and a commercial flatbed scanner. *Med Phys*. 2011;38:1919–1930.
37. White MC. Further notes on MCPLIB03/04 and new MCPLIB63/84 Compton broadening data for all versions of MCNP5. Tech. Rep. LA-UR-12-00018, Los Alamos National Laboratory (2012).
38. Rosen BS, Soares CG, Hammer CG, Kunugi KA, DeWerd LA. A prototype, glassless densitometer traceable to primary optical standards for quantitative radiochromic dosimetry. *Med Phys*. 2015;42:4055–4068.
39. Menegotti L, Delana A, Martignano A. Radiochromic film dosimetry with flatbed scanners: a fast and accurate method for dose calibration and uniformity correction with single film exposure. *Med Phys*. 2008;35:3078–3085.
40. Saur S, Frengen J. GafChromic EBT film dosimetry with flatbed CCD scanner: a novel background correction method and full dose uncertainty analysis. *Med Phys*. 2008;35:3094–3101.
41. Soares CG. Radiochromic film. In: Rogers DWO, Cygler JE, eds. *Clinical Dosimetry Measurements in Radiotherapy*. Colorado Springs CO: AAPM Summer School, American Association of Physicists in Medicine; 2009. Presentation.
42. Massillon-JL G, Cueva-Prócel D, Díaz-Aguirre P, Rodríguez-Ponce M, Herrera-Martínez F. Dosimetry for small fields in stereotactic radiosurgery using Gafchromic MD-V2-55 film, TLD-100 and alanine dosimeters. *PLoS ONE*. 2013;8:1–8.
43. Piringer O, Baner A. *Plastic Packaging: Interactions with Food and Pharmaceuticals*. Weinheim Chichester: Wiley-VCH; 2008.
44. Devic S, Aldelaijan S, Mohammed H, Tomic N, Liang L, Deblois F, Seuntjens J. Absorption spectra time evolution of EBT-2 model GAFCHROMIC[™] film. *Med Phys*. 2010;37:2207–2214.
45. Martišiková M, Ackermann B, Jäkel O. Analysis of uncertainties in Gafchromic[®] EBT film dosimetry of photon beams. *Phys Med Biol*. 2008;53:7013–7027.
46. Lewis D. Radiochromic film. 2010.
47. McLaughlin WL, Al-Sheikhly M, A Lewis DF, Kováč, Wójnarovits L. Radiochromic solid-state polymerization reaction. In: *Irradiation of Polymers*. Washington, DC: American Chemical Society; 1996:152–166.
48. Taylor BN, Kuyatt CE. Guidelines for evaluating and expressing the uncertainty of NIST measurement results. Technical Note 1297, National Institute of Standards and Technology, 1994.
49. University of Wisconsin Radiation Calibration Laboratory. *UW-RCL Quality Manual 1.3.3 Uncertainty Tables: Air Kerma Therapy*. Madison, WI: UWADCL; 2008.